



# HHS Public Access

Author manuscript

*J Cell Biochem.* Author manuscript; available in PMC 2018 July 01.

Published in final edited form as:

*J Cell Biochem.* 2017 July ; 118(7): 1678–1688. doi:10.1002/jcb.25825.

## Evidence for pipecolate oxidase in mediating protection against hydrogen peroxide stress

Sathish Kumar Natarajan<sup>1,2</sup>, Ezhumalai Muthukrishnan<sup>2</sup>, Oleh Khalimonchuk<sup>1</sup>, Justin L. Mott<sup>3</sup>, and Donald F. Becker<sup>1</sup>

<sup>1</sup>Department of Biochemistry and Redox Biology Center, University of Nebraska-Lincoln, Lincoln, NE, 68588, USA

<sup>2</sup>Department of Nutrition and Health Sciences, University of Nebraska-Lincoln, Lincoln, NE 68583, USA

<sup>3</sup>Department of Biochemistry and Molecular Biology, University of Nebraska Medical Center, Omaha, NE, 68198, USA

### Abstract

Pipecolate, an intermediate of the lysine catabolic pathway, is oxidized to <sup>1</sup>-piperidine-6-carboxylate (P6C) by the flavoenzyme L-pipecolate oxidase (PIPOX). P6C spontaneously hydrolyzes to generate  $\alpha$ -amino adipate semialdehyde, which is then converted into  $\alpha$ -amino adipate acid by  $\alpha$ -amino adipate semialdehyde dehydrogenase. L-pipecolate was previously reported to protect mammalian cells against oxidative stress. Here, we examined whether PIPOX is involved in the mechanism of pipecolate stress protection. Knockdown of PIPOX by small interference RNA abolished pipecolate protection against hydrogen peroxide-induced cell death in HEK293 cells suggesting a critical role for PIPOX. Subcellular fractionation analysis showed that PIPOX is localized in the mitochondria of HEK293 cells consistent with its role in lysine catabolism. Signaling pathways potentially involved in pipecolate protection were explored by treating cells with small molecule inhibitors. Inhibition of both mTORC1 and mTORC2 kinase complexes or inhibition of Akt kinase alone blocked pipecolate protection suggesting the involvement of these signaling pathways. Phosphorylation of the Akt downstream target, forkhead transcription factor O3 (FoxO3), was also significantly increased in cells treated with pipecolate, further implicating Akt in the protective mechanism and revealing FoxO3 inhibition as a potentially key step. The results presented here demonstrate that pipecolate metabolism can influence cell signaling during oxidative stress to promote cell survival and suggest that the mechanism of pipecolate protection parallels that of proline, which is also metabolized in the mitochondria.

**Correspondence:** Donald F. Becker, Department of Biochemistry and Redox Biology Center, University of Nebraska-Lincoln, N258 Beadle Center, Lincoln, NE 68588, Tel. 402-472-9652; Fax. 402-472-7842; dbecker3@unl.edu.

### Author contributions

SKN designed and performed the experiments. EM performed the NADPH/NADP<sup>+</sup> measurements. OK designed and guided the subcellular localization experiments. JLM helped with the signaling pathway analysis. DFB designed and coordinated the overall project and all authors contributed to the writing of the manuscript.

## Keywords

pipecolate; pipecolate oxidase; amino acid metabolism; oxidative stress; mitochondria

L-pipecolic acid is a nonproteinogenic amino acid of lysine metabolism. In humans, pipecolate is derived from the saccharopine branch of lysine catabolism and by an alternative lysine degradation pathway initiated by  $\alpha$ -deamination of lysine [Struys and Jakobs, 2010]. L-pipecolate is oxidized to <sup>1</sup>-piperideine-6-carboxylate (P6C) by the flavoenzyme pipecolate oxidase (PIPOX) (Fig. 1A). Spontaneous hydrolysis of P6C then generates  $\alpha$ -aminoadipate semialdehyde (AAS), an intermediate that is also generated from saccharopine by AAS synthase of the main lysine degradation pathway [Struys and Jakobs, 2010]. AAS is subsequently oxidized by NAD<sup>+</sup>-dependent AAS dehydrogenase (AASDH1, also known as aldehyde dehydrogenase 7A1) [Luo and Tanner, 2015] to form  $\alpha$ -aminoadipic acid (AAA), which is eventually converted to glutaryl-CoA via  $\alpha$ -ketoadipic acid [Struys and Jakobs, 2010].

Human PIPOX is a polypeptide of 390 residues with a molecular weight of 44 kDa and contains a covalently bound flavin cofactor [Dodt et al., 2000]. Characterization of PIPOX from different mammalian sources shows that in addition to oxidizing pipecolate, PIPOX can utilize sarcosine and proline as alternative substrates, albeit with lower efficiency [Dodt et al., 2000; Mihalik et al., 1991]. Elevated pipecolic acid concentration in serum (hyperpipecolic acidemia) is used as a marker of pyridoxine dependent epilepsy and AASDH deficiency [Stockler et al., 2011], and is associated with peroxisome biogenesis disorders such as Zellweger syndrome [Moser et al., 1989; Wanders et al., 1988].

Our interest in L-pipecolic acid is from a previous study in which we tested the ability of proline and proline analogs to protect mammalian cells against oxidative stress. In addition to proline, we found that pipecolate, a six-member proline analog, significantly increased cell survival after exposure to H<sub>2</sub>O<sub>2</sub> stress [Krishnan et al., 2008]. The mechanism by which proline improves cell survival was shown to be mediated by proline dehydrogenase (PRODH) [Natarajan et al., 2012]. PRODH is a mitochondrial enzyme that performs the first step of proline degradation by catalyzing the oxidation of proline to <sup>1</sup>-pyrroline-5-carboxylate (P5C) (Fig. 1B), which is then converted into glutamate by P5C dehydrogenase. Knockdown of PRODH eliminated the protective effect of proline against H<sub>2</sub>O<sub>2</sub> stress [Natarajan et al., 2012]. Additionally, it was shown that proline and PRODH increase activation of Akt signaling during stress suggesting a mechanism for how proline enhances cell survival [Natarajan et al., 2012].

Here we investigate the mechanism of pipecolate protection against H<sub>2</sub>O<sub>2</sub> induced cell death. PIPOX catalyzes the oxidation of L-pipecolate in a reaction analogous to PRODH (Fig. 1A) suggesting that similar to proline, the protective effect of pipecolate may depend on this first oxidative step. The role of PIPOX in pipecolate protection was thus examined and the mechanistic target of rapamycin complex (mTOR) and Akt kinase were explored to test their potential involvement in pipecolate protection. Subcellular localization of PIPOX was also assessed to establish whether PIPOX is expressed in mitochondria. We found that in HEK293 cells a majority of PIPOX localizes to mitochondria and our results suggest that

the mechanism by which pipercolate provides cellular stress protection parallels that of proline.

## MATERIALS AND METHODS

### Materials

Unless stated otherwise, all chemicals, enzymes and buffers were purchased from Fisher Scientific and Sigma-Aldrich, Inc. For this study, we used human embryonic kidney 293 (HEK293) cells purchased from ATCC.

### Antibodies

Antibodies recognizing VDAC/Porin (#V2139) and  $\beta$ -Actin (#A5441) were from Sigma. The monoclonal antibody against PIPOX (PIPOX F-9, #sc-166749) was from Santa-Cruz and anti-catalase antibody (#ab15834) was from Abcam. Antibodies against phospho-Akt T308 (#4056), phospho-Akt S473 (#4058), phospho-JNK (#4668), phospho-FoxO3 (Thr32) (#9464) and total forms of FoxO3 (#2497), Akt (#4685), and JNK (#9252) were from Cell Signaling Technology. Horseradish peroxidase-labeled anti-mouse (#NA931), and anti-rabbit (#RPN4301) secondary antibodies were from GE Healthcare.

### Stress tests and cell viability

HEK293 cells were grown in Dulbecco's Modified Eagle's Medium (DMEM) supplemented with 10% FBS and penicillin-streptomycin (100 U/ml). For stress treatments, HEK293 were grown to 80% confluence and then pretreated with and without L-pipercolate in serum containing medium for 12 h. After the pretreatment period, cells were exposed to H<sub>2</sub>O<sub>2</sub> (50 and 500  $\mu$ M) for 3 h in serum free medium with and without L-pipercolate. The protective effect of pipercolate was initially tested with different pipercolate concentrations (0.05–10 mM) and then 1, 5 and 10 mM L-pipercolate were used in subsequent experiments. After stress treatment, cell viability was quantified using the tetrazolium compound [3-(4, 5-dimethylthiazol-2-yl)-5-(3-carboxymethoxyphenyl)-2-(4-sulfophenyl)-2H-tetrazolium] (MTS) according to the recommendation of the manufacturers (Promega). The CellTiter-Glo Luminescent assay (Promega) was also used as an alternative method according to the recommendation of the manufacturers. Percent cell survival was determined relative to the appropriate controls. Stress tests with proline were performed similarly to pipercolate but using 5 mM L-proline. Stress tests were also performed in the presence of different inhibitor compounds. To inhibit the pentose phosphate pathway, HEK293 cells were incubated with 6-aminonicotinamide (6-AN) (50  $\mu$ M) or dehydroepiandrosterone (DHEA) (50  $\mu$ M) for 24 h before adding pipercolate (10 mM) to the cell culture. After 12 h incubation with pipercolate, cells were then treated with H<sub>2</sub>O<sub>2</sub> as described above. Inhibition of the mechanistic target of rapamycin (mTOR) pathway was achieved by incubating HEK293 cells with rapamycin (Calbiochem) at 10 nM and 100 nM concentrations for 2 h prior to H<sub>2</sub>O<sub>2</sub> stress. Inhibition of both mTORC1 and mTORC2 was achieved by incubating HEK293 cells with 10 nM of KU-0063794 for 2 h prior to H<sub>2</sub>O<sub>2</sub> stress. To inhibit Akt activity, HEK293 were treated with 10  $\mu$ M Akt Inhibitor VIII (Akti-Calbiochem), which selectively inhibits Akt1/Akt2 activity, for 30 min prior to H<sub>2</sub>O<sub>2</sub> stress. Stock solutions of the inhibitor compounds DHEA, 6-AN, rapamycin, and Akti were prepared in dimethyl sulfoxide (DMSO).

### G6PDH assay and NADPH measurements

Glucose-6-phosphate dehydrogenase (G6PDH) activity was measured according to the recommendation of the manufacturer (BioVision). One unit of enzyme is defined as 1  $\mu\text{mol}$  of product formed per min at 37 °C. Total protein concentration in the cell lysates was determined using the bicinchoninic acid (BCA) protein assay (Pierce) using bovine serum albumin as a standard. Cellular NADPH/NADP<sup>+</sup> (MilliporeSigma) levels were estimated as previously described according to the manufacturer's recommendation [Natarajan et al., 2012].

### Western blot analysis

Cells grown in 10 cm diameter dishes were rinsed once with ice cold PBS and cell lysates were prepared using M-PER according to the recommendation of the manufacturers along with the addition of mammalian protease inhibitor cocktail (Sigma) and HALT-phosphatase inhibitor (Pierce). Lysates containing 50–100  $\mu\text{g}$  of protein were resolved by SDS-PAGE. Proteins were transferred to a PVDF membrane and visualized by immunoblotting.

### Mitochondrial isolation

Cells were released with trypsin and washed twice via centrifugation with ice cold PBS. Cell pellets were then resuspended in Tris buffer (5 mM, pH 7.4) containing 0.25 M sucrose, 1 mM EDTA, and mammalian protease inhibitor cocktail (Sigma). The resuspended cells were next hand homogenized using a dounce homogenizer for 1 min on ice. Mitochondria and cytosolic fractions were isolated by differential centrifugation as described [Natarajan et al., 2006a]. Briefly, cell homogenates were first centrifuged at  $600 \times g$  for 10 min to remove cell debris. Mitochondria were then pelleted at  $17,000 \times g$  for 15 min (4 °C) and washed twice with mitochondrial suspension buffer (5 mM Tris, pH 7.4, 0.25 M sucrose). The post-mitochondrial supernatant was then centrifuged at  $32,000 \times g$  for 20 min to isolate the peroxisome fraction [Natarajan et al., 2006a]. The peroxisomal fraction was resuspended in the mitochondrial suspension buffer and then centrifuged at  $17,000 \times g$  for 15 min to remove mitochondria. The supernatant was then centrifuged again at  $32,000 \times g$  for 20 min to collect pure peroxisomes [Natarajan et al., 2006a; Natarajan et al., 2006b]. The post-peroxisomal supernatant was centrifuged at  $105,000 \times g$  for 1 h to isolate the cytosolic fraction [Natarajan et al., 2006a]. Density-purified mitochondria were isolated on a discontinuous Histodenz [5-(N-2,3-Dihydroxy propylacetamido)-2,4,6-triiodo-N,N'-bis(2,3-dihydroxypropyl)isophthalamide] gradient as described [Atkinson et al., 2011; Boldogh and Pon, 2007]. Briefly, the mitochondria-enriched fraction obtained from differential centrifugation was layered onto a discontinuous Histodenz gradient consisting of 14% and 22% layers dissolved in sorbitol buffer. Histodenz gradients were centrifuged at  $303,000 \times g$  for 1 h [Atkinson et al., 2011]. Mitochondrial fractions were then resuspended in mitochondrial suspension buffer and used for Western blot analysis. Total protein concentrations were quantified using the Bradford method (Bio-Rad).

### siRNA transfection

Cells were transfected with On-Target Plus Smart Pool siRNA of PIPOX and On-Target Plus Non-targeting Pool, referred to as control siRNA (Dharmacon RNA Technologies). siRNA

transfection was performed for 48 h before doing the stress test or whole cell extract collection. Knockdown was confirmed by immunoblotting. Following transfection, stress tests were performed as described above.

### Statistical analysis

Data are expressed as mean  $\pm$  standard deviation (SD). Statistical analysis was performed using student's t-test. A *P* value of  $<0.05$  was considered to be statistically significant.

## RESULTS

### Pipecolate protects HEK293 cells

Pipecolate was previously shown to protect HEK293 cells against H<sub>2</sub>O<sub>2</sub>-induced cell death [Krishnan et al., 2008]. Here we pretreated HEK293 cells with different concentrations of pipecolate (0.05–10 mM) for 12 h prior to H<sub>2</sub>O<sub>2</sub> stress treatment (0.5 mM, 3 h). Pipecolate protected HEK293 cells against oxidative stress with significant protection observed at 0.75 mM pipecolate relative to control cells without pipecolate supplementation (Fig. 2A, B) [Krishnan et al., 2008]. The protective effect of pipecolate was also investigated using luminescence quantification of ATP generation. In these assays, pipecolate increased cell survival in HEK293 cells (Fig. 2C) from 40% to 74%.

Pipecolate protection was also examined at a more pathophysiology-relevant level of oxidative stress by using a lower concentration of H<sub>2</sub>O<sub>2</sub>. At 50  $\mu$ M H<sub>2</sub>O<sub>2</sub> (3 h), percent cell survival was significantly higher in HEK293 cells treated with pipecolate relative to control cells without pipecolate (Fig. 2D). Thus, pipecolate was able to protect cells against a H<sub>2</sub>O<sub>2</sub> concentration that more closely mimics pathophysiological stress.

### PIPOX knockdown by siRNA

We next examined the effect of reducing endogenous PIPOX expression by transfecting HEK293 cells with PIPOX siRNA (siPIPOX). Knockdown of PIPOX expression was confirmed by Western blot analysis of whole cell lysates. PIPOX expression was observed to be significantly lower in HEK293 cells after 48 h of siPIPOX treatment relative to cells treated with control siRNA (Fig. 3A). In siPIPOX-transfected cells, pipecolate protection against H<sub>2</sub>O<sub>2</sub>-induced cell death was eliminated whereas in control siRNA treated cells pipecolate protection was still observed (Fig. 3B). Pipecolate (1–5 mM) was also unprotective in siPIPOX-transfected cells exposed to pathophysiological levels of H<sub>2</sub>O<sub>2</sub> (50  $\mu$ M) (Fig. 3C). Next, we tested whether proline supplementation could protect against H<sub>2</sub>O<sub>2</sub> stress in cells treated with PIPOX siRNA. Proline significantly increased survival of HEK293 cells treated with PIPOX siRNA (Fig. 3D). These results show that although PIPOX can utilize proline as an alternative substrate, PIPOX is not essential for proline protection. Thus, it appears PIPOX is necessary for pipecolate protection.

### PIPOX subcellular localization

Because PIPOX was observed to be essential for pipecolate protection, we sought to establish the subcellular localization of PIPOX in HEK293 cells. Human PIPOX terminates at the C-terminus with an Ala-His-Leu tripeptide peroxisome targeting signal [L et al.,

2000], however, PIPOX has been shown previously to localize to the peroxisomes and the mitochondria depending on the species [L et al., 2000]. Western analysis of PIPOX expression in the different subcellular compartments was performed using highly purified mitochondria, peroxisomes, and cytosolic fractions from HEK293 cells. Figure 4 shows that PIPOX was detected predominantly in isolated mitochondria. To check whether the purified mitochondria were contaminated with peroxisomes, we tested for the presence of catalase. High expression levels of catalase were observed in the peroxisomal fraction whereas catalase was not detected in the mitochondria indicating that the purified mitochondria were not contaminated with peroxisomes (Figure 4).

### NADPH/NADP<sup>+</sup> and pentose phosphate pathway

The effect of pipercolate on the NADPH/NADP<sup>+</sup> ratio was measured in cells before and after H<sub>2</sub>O<sub>2</sub> stress. The cellular NADPH/NADP<sup>+</sup> ratio in HEK293 cells decreased in control cells after 3 h of 500 μM H<sub>2</sub>O<sub>2</sub> stress (Fig. 5A). In cells treated with pipercolate, however, the NADPH/NADP<sup>+</sup> ratio increased during H<sub>2</sub>O<sub>2</sub> stress resulting in a ~ 5-fold higher ratio than in control cells (Fig. 5A). Next, we tested whether increased NADPH/NADP<sup>+</sup> ratio with pipercolate treatment is via activating pentose phosphate pathway. Cells were treated with 6-aminonicotinamide (6-AN) and dehydroepiandrosterone (DHEA), which inhibit glucose 6-phosphate dehydrogenase (G6PDH) of the pentose phosphate pathway. Treatment of cells with 6AN and DHEA showed a significant decrease in G6PDH activity (Fig. 5B) while the pipercolate-induced increase in the NADPH/NADP<sup>+</sup> ratio was abolished in cells treated with the inhibitors (Fig 5A). Further, we also tested the effect of pipercolate protection during inhibition of pentose phosphate pathway. Interestingly, pipercolate protection of HEK293 cells was still observed in the presence of the 6-AN and DHEA indicating that the pentose phosphate pathway is not critical in these H<sub>2</sub>O<sub>2</sub> stress experiments (Fig. 5C and D).

### Inhibition of mTORC

The mechanistic target of rapamycin complex 1 (mTORC1) is known to be activated by amino acids [Lynch, 2001; Zoncu et al., 2011] and we recently discovered a role for mTORC in proline protection [Natarajan et al., 2012]. To test whether mTORC1 and mTORC2 are also involved in pipercolate protection, HEK293 cells were incubated with 10 nM rapamycin, a concentration previously shown to inhibit mTORC1 in cells [Lasithiotakis et al., 2008]. Treatment of cells with rapamycin did not attenuate pipercolate protection against H<sub>2</sub>O<sub>2</sub> stress in HEK293 cells (Fig. 6A) suggesting that mTORC1 is not involved. Treating cells with a higher concentration of rapamycin (100 nM), which inhibits mTORC1 and the Rictor-complex of mTOR (mTORC2) [Sarbasov et al., 2006], abrogated pipercolate protection (Fig. 6A) implying that mTORC2 may be involved. This was further tested by treating HEK293 cells with 10 nM of KU-0063794, which also inhibits mTORC1 and mTORC2. Similar to using a high concentration of rapamycin, treatment of cells with KU-0063794 abolished pipercolate protection against H<sub>2</sub>O<sub>2</sub> stress, suggesting a role for mTORC2 in pipercolate protection (Fig. 6B).

### Role of Akt and FoxO3 during H<sub>2</sub>O<sub>2</sub> stress

Akt/PKB (Protein kinase B) can significantly impact cell survival and proliferation and, is a downstream target of mTORC2 [Altomare and Khaled, 2012; Berndt et al., 2010]. Cells



were treated with the Akt inhibitor, Akti, to test the involvement of Akt in pipecolate protection [Calleja et al., 2009]. At different concentrations of pipecolate (1 and 10 mM), Akti was observed to block pipecolate protection of HEK293 cells against H<sub>2</sub>O<sub>2</sub> stress (Fig. 7A). Akti inhibition of Akt was confirmed by loss of phosphorylation at Akt residues T308 and S473 as shown in Figure 7B. Exposure of control cells to H<sub>2</sub>O<sub>2</sub> increases phospho-Akt slightly at T308 and more significantly at S473 (Fig. 7B, -Akti). In the absence of H<sub>2</sub>O<sub>2</sub>, pipecolate does not increase the levels of phospho-Akt at T308 and S473 relative to control cells (Fig. 7B, -Akti). However, in the presence of H<sub>2</sub>O<sub>2</sub>, pipecolate appears to significantly increase the levels of phospho-Akt at S473 (Fig. 7B–D, -Akti). Treatment of cells with Akti abolished phosphorylation of Akt under all conditions consistent with inhibition of the Akt signaling pathway (Fig. 7B–D, +Akti). In these experiments, no changes in the levels of total-Akt and the actin control were observed (Fig. 7B). The effects of Akti on other stress signaling pathways such as c-Jun N-terminal Kinase (JNK) were also examined. Akti did not perturb the phosphorylation status of JNK (Fig. 7E).

Activation of Akt can lead to phosphorylation of several transcription factors including the forkhead transcription factor O3 (FoxO3). To test the downstream effects of Akt in pipecolate protection, phosphorylation of FoxO3 (Thr32) was examined after 0.5 and 3 h of H<sub>2</sub>O<sub>2</sub> stress in cells with or without pipecolate. In control cells, a slight increase in phospho-FoxO3 levels was observed with 0.5 h of H<sub>2</sub>O<sub>2</sub> treatment (Fig. 8A, B). A much more dramatic increase in phospho-FoxO3, however, was observed with H<sub>2</sub>O<sub>2</sub> (0.5 h) in the presence of pipecolate (Fig. 8A, B). Addition of Akti (+ Akti) eliminated phosphorylation of FoxO3 indicating involvement of the Akt pathway (Fig. 8A, B). At 3 h of H<sub>2</sub>O<sub>2</sub> treatment, phospho-FoxO3 levels remained slightly higher in pipecolate cells relative to control cells (Fig. 8C). These results suggest increased phosphorylation of FoxO3 is part of the mechanism by which pipecolate protects cells against oxidative stress.

## DISCUSSION

Here we show that PIPOX is required for the observed effects of pipecolate, a finding which is analogous to the role of PRODH in proline protection [Natarajan et al., 2012]. The specificity of proline and pipecolate protection is governed by PRODH and PIPOX, respectively. Although PIPOX can use proline as a substrate, knockdown of PIPOX does not affect proline protection consistent with PRODH being the key proline catabolic enzyme. Conversely, pipecolate is not expected to be a substrate for PRODH [Zhu et al., 2002]. The mutual protective effects of proline and pipecolate, both of which are transported into mammalian cells via the sodium dependent IMINO transporter and the system IMINO transporter 1 [Kowalczyk et al., 2005; Takanaga et al., 2005], are likely due to the analogous flavin-dependent catalyzed reactions of PRODH and PIPOX in mitochondria. The oxidation of these related amino acids involves reduction of a flavin cofactor and subsequent electron transfer from the reduced flavin to an electron acceptor. PRODH is a mitochondrial enzyme that couples the oxidation of proline to reduction of the ubiquinone pool in the mitochondrial membrane (Fig. 1) [Liu et al., 2012; Wanduragala et al., 2010]. PRODH activity has been reported to generate reactive oxygen species (ROS) leading to either cell survival or cell death [Liu et al., 2012; Natarajan and Becker, 2012; Zarse et al., 2012; Zhang et al., 2015]. Here, we show that PIPOX is also predominantly localized in the mitochondria.

Whether PIPOX transfers electrons directly to the mitochondrial electron transport chain is not clear but PIPOX has been shown to generate H<sub>2</sub>O<sub>2</sub> during catalytic turnover [Mihalik et al., 1991; Wanders et al., 1989]. Energy metabolism in the mitochondria is a potent source of ROS, which has been shown to have a plethora of effects on cell proliferation, death, and other growth processes [Figueira et al., 2013; Natarajan and Becker, 2012]. We found that pipecolate shifts the redox status of the NADPH/NADP<sup>+</sup> and helps maintain cellular NADPH/NADP<sup>+</sup> ratios during stress consistent with PIPOX having a role in redox homeostasis. However, the increased NADPH/NADP<sup>+</sup> ratio and pentose phosphate pathway were found not be critical for pipecolate protection against H<sub>2</sub>O<sub>2</sub> stress. Further studies are underway to elucidate the mechanism by which pipecolate influences the redox environment during oxidative stress.

Finding that PIPOX was mainly localized in mitochondria of HEK293 cells was unexpected. Previous studies of PIPOX in rat and human liver detected PIPOX activity in both mitochondria and peroxisomes [Rao et al., 1993; Wanders et al., 1989]. The subcellular localization of PIPOX has been shown to be species-dependent with localization in the peroxisomes suggested to predominate in humans [Mihalik and Rhead, 1989; Mihalik and Rhead, 1991]. In human fibroblasts overexpression of PIPOX resulted in localization of PIPOX in the peroxisomes as detected by immunofluorescence staining [L et al., 2000]. Currently known peroxisomal targeting signals (PTS) are the C-terminal PTS-1 and the N-terminal PTS-2 [Gould and Collins, 2002; Wolf et al., 2010]. PIPOX has a PTS-1 sequence of Ala-His-Leu and does not have a mitochondrial target sequence [L et al., 2000]. Bioinformatics analysis of PIPOX using MitoProt [Claros and Vincens, 1996], a program that does not rely on identifying a targeting peptide but instead evaluates up to 47 parameters, gives a low probability (MitoProt score of 15%) for PIPOX import into mitochondria despite PIPOX not having a mitochondrial targeting sequence. Another bioinformatics tool, WoLF PSORT [Horton et al., 2007], predicts that PIPOX is favored to be localized in the mitochondria rather than in the peroxisomes. It is established that peroxisomal targeting sequences do not necessarily limit protein localization to the peroxisomes [Wolf et al., 2010]. In addition, it is becoming more recognized that proteins can be located in more than one compartment [Hogenboom et al., 2004; Islinger et al., 2012; O'Byrne et al., 2003; Taylor et al., 2004; Yogev and Pines, 2011]. Dual localization of proteins can occur by various mechanisms involving two target signals in a single polypeptide and target signals that are inaccessible or ambiguous [Hogenboom et al., 2004; Islinger et al., 2012; O'Byrne et al., 2003; Taylor et al., 2004; Yogev and Pines, 2011].

Mitochondrial localization of PIPOX in HEK293 cells is consistent with its role in the lysine catabolic pathway, which involves mitochondrial enzymes such as AASDH (also known as ALDH7A1) [Brockner et al., 2010; Luo and Tanner, 2015; Stockler et al., 2011; Struys and Jakobs, 2010]. Recently, PIPOX was suggested to function as a metabolic repair enzyme by minimizing pipecolate accumulation and increasing the overall conversion of lysine to glutaryl-CoA [Struys and Jakobs, 2010; Van Schaftingen et al., 2013]. Pyrroline-5-carboxylate reductase (P5CR) has been proposed to catalyze the NADPH-dependent reduction of P6C to pipecolate as a side reaction thereby diminishing lysine catabolic efficiency [Struys and Jakobs, 2010; Van Schaftingen et al., 2013]. The preferred substrate for P5CR is <sup>1</sup>-pyrroline-5-carboxylate, but P5CR from *Escherichia coli* has been shown to



convert P6C to pipecolate [Fujii et al., 2002]. Humans have three isoforms of P5CR known as PYCR1, PYCR2, and PYCRL [De Ingeniis et al., 2012; Reversade et al., 2009]. PYCR1 and PYCR2 were recently shown to localize in the mitochondria [De Ingeniis et al., 2012; Reversade et al., 2009]. Finding that PIPOX is also localized in the mitochondria further supports a repair role for PIPOX, which merits future investigation.

The results here with pipecolate and previously with proline [Natarajan et al., 2012], indicate that the protective effects of these amino acids involve the Akt and its downstream mediators. In the previous study with proline, PRODH was shown to increase Akt phosphorylation (Ser473) and phosphorylation of the Akt downstream target, FoxO3 [Natarajan et al., 2012]. Phosphorylation of FoxO3 by Akt prevents activation of pro-apoptotic genes thus promoting cell survival [Guo et al., 2011]. In this study, inhibition of Akt abolished phosphorylation of FoxO3 and the protective effect of pipecolate. Thus, the protective mechanism of pipecolate appears to be mediated by Akt and FoxO3. As previously observed with proline, dual inhibition of mTORC complexes, blocks pipecolate protection against oxidative stress. These observations indicate that mTORC2 may be involved in the mechanism of cell protection. mTORC2 has been shown to activate Akt via phosphorylation of Ser473 [Guo et al., 2011; Murata et al., 2011]. How pipecolate and proline influence mTORC2 and Akt signaling is not clear but amino acids have been shown to induce mTORC1 and mTORC2 in mammalian cells [Tato et al., 2011]. In addition, evidence has been reported for mTORC2 being activated by mitochondrial ROS suggesting that the intracellular redox environment modulates mTORC2 [Kumari Kanchan et al., 2012]. Whether ROS is a key mediator by which proline and pipecolate metabolism mediate mTORC2 and Akt pathway activity remains to be determined.

In summary, we show that pipecolate metabolism leads to protection against H<sub>2</sub>O<sub>2</sub> stress in mammalian cells. Our findings expand the potential role of pipecolate metabolism in mediating cell signaling. Previous studies reporting that pipecolate impacts oxidative stress were focused on exploring the role of pipecolate in neurological function. Incubation of rat cerebral cortex supernatants with pipecolate for 1 h was shown to decrease the activity of antioxidant enzymes, an effect that could be blocked by lipoic acid [Dalazen et al., 2014]. Pipecolate was also shown to stimulate apoptotic cell death in neurons [Matsumoto et al., 2003]. Treatment of mouse neuroblastoma cells with D- or L-pipecolate over 72 h decreased cell viability with a racemic mixture of DL-pipecolate having the most toxic effect [Matsumoto et al., 2003]. Because D-pipecolate decreased cell viability, the mechanism appears to be independent of pipecolate oxidase activity, which is specific for L-pipecolate [Matsumoto et al., 2003]. Different roles for D- and L-pipecolate have also been found in other biological contexts such as L-pipecolate acting as an anti-hypertensive by competitively inhibiting the angiotensin I-converting enzyme, whereas, the D-enantiomer does not have an antihypertensive function [Vranova et al., 2013]. Future studies will investigate the protective role of pipecolate metabolism and downstream pathways involving mTORC2, Akt and FoxO3 using other cell types to broaden our understanding of how pipecolate impacts the cellular redox environment.

## Acknowledgments

We thank Dr. Nishikant Wase for his help with the bioinformatics analysis of PIPOX. This research was supported in part by grants P20GM104320 to SKN and JLM, and GM079393 and P30GM103335 to DFB from the National Institutes of Health.

## Abbreviations

<b>AAA</b>	$\alpha$ -aminoadipic acid
<b>AAS</b>	$\alpha$ -AAA semialdehyde
<b>AASDH</b>	$\alpha$ -AAS dehydrogenase
<b>6AN</b>	6-aminonicotinamide
<b>DHEA</b>	dehydroepiandrosterone
<b>DMSO</b>	dimethyl sulfoxide
<b>FoxO</b>	fork head family of transcription factor class O
<b>G6PDH</b>	glucose-6-phosphate dehydrogenase
<b>GSA</b>	glutamate $\gamma$ -semialdehyde
<b>HEK293</b>	human embryonic kidney 293
<b>mTORC</b>	mammalian target of rapamycin complex
<b>MTS</b>	[3-(4,5-dimethylthiazol-2-yl)-5-(3-carboxymethoxyphenyl)-2-(4-sulfophenyl)-2H-tetrazolium]
<b>PTS</b>	peroxisomal targeting signal
<b>PIPOX</b>	pipecolate oxidase
<b>P6C</b>	<sup>1</sup> -piperidine-6-carboxylate
<b>PRODH</b>	proline dehydrogenase
<b>P5C</b>	<sup>1</sup> -pyrroline-5-carboxylate
<b>P5CDH</b>	P5C dehydrogenase
<b>P5CR</b>	P5C reductase
<b>VDAC</b>	voltage-dependent anion channel

## References

- Altomare DA, Khaled AR. Homeostasis and the importance for a balance between AKT/mTOR activity and intracellular signaling. *Curr Med Chem.* 2012; 19:3748–3762. [PubMed: 22680924]
- Atkinson A, Smith P, Fox JL, Cui TZ, Khalimonchuk O, Winge DR. The LYR protein Mzm1 functions in the insertion of the Rieske Fe/S protein in yeast mitochondria. *Mol Cell Biol.* 2011; 31:3988–3996. [PubMed: 21807901]

- Berndt N, Yang H, Trinczek B, Betzi S, Zhang Z, Wu B, Lawrence NJ, Pellicchia M, Schonbrunn E, Cheng JQ, Sebti SM. The Akt activation inhibitor TCN-P inhibits Akt phosphorylation by binding to the PH domain of Akt and blocking its recruitment to the plasma membrane. *Cell Death Differ.* 2010; 17:1795–1804. [PubMed: 20489726]
- Boldogh IR, Pon LA. Purification and subfractionation of mitochondria from the yeast *Saccharomyces cerevisiae*. *Methods Cell Biol.* 2007; 80:45–64. [PubMed: 17445688]
- Brocker C, Lassen N, Estey T, Pappa A, Cantore M, Orlova VV, Chavakis T, Kavanagh KL, Oppermann U, Vasiliou V. Aldehyde dehydrogenase 7A1 (ALDH7A1) is a novel enzyme involved in cellular defense against hyperosmotic stress. *J. Biol. Chem.* 2010; 285:18452–18463. [PubMed: 20207735]
- Calleja V, Laguerre M, Parker PJ, Larijani B. Role of a novel PH-kinase domain interface in PKB/Akt regulation: structural mechanism for allosteric inhibition. *PLoS Biol.* 2009; 7:e17. [PubMed: 19166270]
- Claros MG, Vincens P. Computational method to predict mitochondrially imported proteins and their targeting sequences. *Eur J Biochem.* 1996; 241:779–786. [PubMed: 8944766]
- Dalazen GR, Terra M, Jacques CE, Coelho JG, Freitas R, Mazzola PN, Dutra-Filho CS. Pipecolic acid induces oxidative stress in vitro in cerebral cortex of young rats and the protective role of lipoic acid. *Metab Brain Dis.* 2014; 29:175–183. [PubMed: 24338030]
- De Ingeniis J, Ratnikov B, Richardson AD, Scott DA, Aza-Blanc P, De SK, Kazanov M, Pellicchia M, Ronai Z, Osterman AL, Smith JW. Functional specialization in proline biosynthesis of melanoma. *Plos One.* 2012; 7
- Dotd G, Kim DG, Reimann SA, Reuber BE, McCabe K, Gould SJ, Mihalik SJ. L-Pipecolic acid oxidase, a human enzyme essential for the degradation of L-pipecolic acid, is most similar to the monomeric sarcosine oxidases. *Biochem. J.* 2000; 345(Pt 3):487–494. [PubMed: 10642506]
- Figueira TR, Barros MH, Camargo AA, Castilho RF, Ferreira JC, Kowaltowski AJ, Sluse FE, Souza-Pinto NC, Vercesi AE. Mitochondria as a source of reactive oxygen and nitrogen species: From molecular mechanisms to human health. *Antioxid Redox Signal.* 2013; 18:2029–2074. [PubMed: 23244576]
- Fujii T, Mukaiyama M, Agematu H, Tsunekawa H. Biotransformation of L-lysine to L-pipecolic acid catalyzed by L-lysine 6-aminotransferase and pyrroline-5-carboxylate reductase. *Biosci. Biotech. Biochem.* 2002; 66:622–627.
- Gould SJ, Collins CS. Opinion: peroxisomal-protein import: is it really that complex? *Nat Rev Mol Cell Biol.* 2002; 3:382–389. [PubMed: 11988772]
- Guo JP, Coppola D, Cheng JQ. IKBKE protein activates Akt independent of phosphatidylinositol 3-kinase/PDK1/mTORC2 and the pleckstrin homology domain to sustain malignant transformation. *J. Biol. Chem.* 2011; 286:37389–37398. [PubMed: 21908616]
- Hogenboom S, Tuyp JJM, Espeel M, Koster J, Wanders RJA, Waterham HR. Mevalonate kinase is a cytosolic enzyme in humans. *J. Cell Sci.* 2004; 117:631–639. [PubMed: 14730012]
- Horton P, Park KJ, Obayashi T, Fujita N, Harada H, Adams-Collier CJ, Nakai K. WoLF PSORT: protein localization predictor. *Nucleic Acids Res.* 2007; 35:W585–W587. [PubMed: 17517783]
- Islinger M, Grille S, Fahimi HD, Schrader M. The peroxisome: an update on mysteries. *Histochem Cell Biol.* 2012; 137:547–574. [PubMed: 22415027]
- Kowalczyk S, Broer A, Munzinger M, Tietze N, Klingel K, Broer S. Molecular cloning of the mouse IMINO system: an Na<sup>+</sup>- and Cl<sup>-</sup>-dependent proline transporter. *Biochem. J.* 2005; 386:417–422. [PubMed: 15689184]
- Krishnan N, Dickman MB, Becker DF. Proline modulates the intracellular redox environment and protects mammalian cells against oxidative stress. *Free Radic. Biol. Med.* 2008; 44:671–681. [PubMed: 18036351]
- Kumari Kanchan R, Tripathi C, Singh Baghel K, Kumar Dwivedi S, Kumar B, Sanyal S, Sharma S, Mitra K, Garg V, Singh K, Sultana S, Kamal Tripathi R, Kumar Rath S, Bhaduria S. Estrogen receptor potentiates mTORC2 signaling in breast cancer cells by upregulating superoxide anions. *Free Radic Biol Med.* 2012; 53:1929–1941. [PubMed: 23000059]

- L IJ, de Kromme I, Oostheim W, Wanders RJ. Molecular cloning and expression of human L-pipecolate oxidase. *Biochem. Biophys. Res. Commun.* 2000; 270:1101–1105. [PubMed: 10772957]
- Lasithiotakis KG, Sinnberg TW, Schittek B, Flaherty KT, Kulms D, Maczey E, Garbe C, Meier FE. Combined inhibition of MAPK and mTOR signaling inhibits growth, induces cell death, and abrogates invasive growth of melanoma cells. *J Invest Dermatol.* 2008; 128:2013–2023. [PubMed: 18323781]
- Liu W, Le A, Hancock C, Lane AN, Dang CV, Fan TWM, Phang JM. Reprogramming of proline and glutamine metabolism contributes to the proliferative and metabolic responses regulated by oncogenic transcription factor c-MYC. *Proc. Nat. Acad. Sci. USA.* 2012; 109:8983–8988. [PubMed: 22615405]
- Luo M, Tanner JJ. Structural Basis of Substrate Recognition by Aldehyde Dehydrogenase 7A1. *Biochemistry.* 2015; 54:5513–5522. [PubMed: 26260980]
- Lynch CJ. Role of leucine in the regulation of mTOR by amino acids: revelations from structure-activity studies. *J. Nutr.* 2001; 131:861S–865S. [PubMed: 11238775]
- Matsumoto S, Yamamoto S, Sai K, Maruo K, Adachi M, Saitoh M, Nishizaki T. Pipecolic acid induces apoptosis in neuronal cells. *Brain Res.* 2003; 980:179–184. [PubMed: 12867256]
- Mihalik SJ, McGuinness M, Watkins PA. Purification and characterization of peroxisomal L-pipecolic acid oxidase from monkey liver. *J. Biol. Chem.* 1991; 266:4822–4830. [PubMed: 2002029]
- Mihalik SJ, Rhead WJ. L-pipecolic acid oxidation in the rabbit and cynomolgus monkey. Evidence for differing organellar locations and cofactor requirements in each species. *J. Biol. Chem.* 1989; 264:2509–2517. [PubMed: 2914918]
- Mihalik SJ, Rhead WJ. Species variation in organellar location and activity of L-pipecolic acid oxidation in mammals. *J. Comp. Physiol. B.* 1991; 160:671–676. [PubMed: 2045546]
- Moser HW, Mihalik SJ, Watkins PA. Adrenoleukodystrophy and other peroxisomal disorders that affect the nervous-system, including new observations on L-pipecolic acid oxidase in primates. *Brain Dev.* 1989; 11:80–90. [PubMed: 2653074]
- Murata H, Sakaguchi M, Jin Y, Sakaguchi Y, Futami J, Yamada H, Kataoka K, Huh NH. A new cytosolic pathway from a Parkinson disease-associated kinase, BRPK/PINK1: activation of AKT via mTORC2. *J Biol Chem.* 2011; 286:7182–7189. [PubMed: 21177249]
- Natarajan SK, Becker DF. Role of apoptosis-inducing factor, proline dehydrogenase, and NADPH oxidase in apoptosis and oxidative stress. *Cell Health Cytoskelet.* 2012; 2012:11–27. [PubMed: 22593641]
- Natarajan SK, Eapen CE, Pullimood AB, Balasubramanian KA. Oxidative stress in experimental liver microvesicular steatosis: role of mitochondria and peroxisomes. *J. Gastroenterol. Hepatol.* 2006a; 21:1240–1249. [PubMed: 16872304]
- Natarajan SK, Eapen CE, Pullimood AB, Balasubramanian KA. Oxidative stress in experimental liver microvesicular steatosis: role of mitochondria and peroxisomes. *J Gastroenterol Hepatol.* 2006b; 21:1240–1249. [PubMed: 16872304]
- Natarajan SK, Zhu W, Liang X, Zhang L, Demers AJ, Zimmerman MC, Simpson MA, Becker DF. Proline dehydrogenase is essential for proline protection against hydrogen peroxide-induced cell death. *Free Radic. Biol. Med.* 2012; 53:1181–1191. [PubMed: 22796327]
- O'Byrne J, Hunt MC, Rai DK, Saeki M, Alexson SE. The human bile acid-CoA:amino acid N-acyltransferase functions in the conjugation of fatty acids to glycine. *J. Biol. Chem.* 2003; 278:34237–34244. [PubMed: 12810727]
- Rao VV, Tsai MJ, Pan XM, Chang YF. L-Pipecolic acid oxidation in rat - subcellular-localization and developmental-study. *Biochim. Biophys. Acta.* 1993; 1164:29–35. [PubMed: 8518295]
- Reversade B, Escande-Beillard N, Dimopoulou A, Fischer B, Chng SC, Li Y, Shboul M, Tham PY, Kayserili H, Al-Gazali L, Shahwan M, Brancati F, Lee H, O'Connor BD, Schmidt-von Kegler M, Merriman B, Nelson SF, Masri A, Alkazaleh F, Guerra D, Ferrari P, Nanda A, Rajab A, Markie D, Gray M, Nelson J, Grix A, Sommer A, Savarirayan R, Janecke AR, Steichen E, Sillence D, Hausser I, Budde B, Nurnberg G, Nurnberg P, Seemann P, Kunkel D, Zambruno G, Dallapiccola B, Schuelke M, Robertson S, Hamamy H, Wollnik B, Van Maldergem L, Mundlos S, Kornak U.

- Mutations in PYCR1 cause cutis laxa with progeroid features. *Nat. Genet.* 2009; 41:1016–1021. [PubMed: 19648921]
- Sarbasov DD, Ali SM, Sengupta S, Sheen JH, Hsu PP, Bagley AF, Markhard AL, Sabatini DM. Prolonged rapamycin treatment inhibits mTORC2 assembly and Akt/PKB. *Mol. Cell.* 2006; 22:159–168. [PubMed: 16603397]
- Stockler S, Plecko B, Gospe SM Jr, Coulter-Mackie M, Connolly M, van Karnebeek C, Mercimek-Mahmutoglu S, Hartmann H, Scharer G, Struijs E, Tein I, Jakobs C, Clayton P, Van Hove JL. Pyridoxine dependent epilepsy and antiquitin deficiency: clinical and molecular characteristics and recommendations for diagnosis, treatment and follow-up. *Mol. Genet. Metab.* 2011; 104:48–60. [PubMed: 21704546]
- Struys EA, Jakobs C. Metabolism of lysine in alpha-amino adipic semialdehyde dehydrogenase-deficient fibroblasts: evidence for an alternative pathway of pipercolic acid formation. *FEBS Lett.* 2010; 584:181–186. [PubMed: 19932104]
- Takanaga H, Mackenzie B, Suzuki Y, Hediger MA. Identification of mammalian proline transporter SIT1 (SLC6A20) with characteristics of classical system imino. *J. Biol. Chem.* 2005; 280:8974–8984. [PubMed: 15632147]
- Tato I, Bartrons R, Ventura F, Rosa JL. Amino acids activate mammalian target of rapamycin complex 2 (mTORC2) via PI3K/Akt signaling. *J. Biol. Chem.* 2011; 286:6128–6142. [PubMed: 21131356]
- Taylor NL, Heazlewood JL, Day DA, Millar AH. Lipoic acid-dependent oxidative catabolism of alpha-keto acids in mitochondria provides evidence for branched-chain amino acid catabolism in Arabidopsis. *Plant Physiol.* 2004; 134:838–848. [PubMed: 14764908]
- Van Schaftingen E, Rzem R, Marbaix A, Collard F, Veiga-da-Cunha M, Linster CL. Metabolite proofreading, a neglected aspect of intermediary metabolism. *J. Inher. Metab. Dis.* 2013; 36:427–434. [PubMed: 23296366]
- Vranova V, Lojkova L, Rejsek K, Formanek P. Significance of the natural occurrence of L- versus D-pipercolic acid: a review. *Chirality.* 2013; 25:823–831. [PubMed: 24114978]
- Wanders RJ, Romeyn GJ, Schutgens RB, Tager JM. L-pipercolate oxidase: a distinct peroxisomal enzyme in man. *Biochem. Biophys. Res. Commun.* 1989; 164:550–555. [PubMed: 2572224]
- Wanders RJ, Romeyn GJ, van Roermund CW, Schutgens RB, van den Bosch H, Tager JM. Identification of L-pipercolate oxidase in human liver and its deficiency in the Zellweger syndrome. *Biochem. Biophys. Res. Commun.* 1988; 154:33–38. [PubMed: 3395335]
- Wanduragala S, Sanyal N, Liang XW, Becker DF. Purification and characterization of Put1p from *Saccharomyces cerevisiae*. *Arch. Biochem. Biophys.* 2010; 498:136–142. [PubMed: 20450881]
- Wolf J, Schliebs W, Erdmann R. Peroxisomes as dynamic organelles: peroxisomal matrix protein import. *FEBS J.* 2010; 277:3268–3278. [PubMed: 20629744]
- Yogev O, Pines O. Dual targeting of mitochondrial proteins: mechanism, regulation and function. *Biochim Biophys Acta.* 2011; 1808:1012–1020. [PubMed: 20637721]
- Zarse K, Schmeisser S, Groth M, Priebe S, Beuster G, Kuhlow D, Guthke R, Platzer M, Kahn CR, Ristow M. Impaired insulin/IGF1 signaling extends life span by promoting mitochondrial L-proline catabolism to induce a transient ROS signal. *Cell Metab.* 2012; 15:451–465. [PubMed: 22482728]
- Zhang L, Alfano JR, Becker DF. Proline metabolism increases katG expression and oxidative stress resistance in *Escherichia coli*. *J. Bacteriol.* 2015; 197:431–440. [PubMed: 25384482]
- Zhu W, Gincherman Y, Docherty P, Spilling CD, Becker DF. Effects of proline analog binding on the spectroscopic and redox properties of PutA. *Arch Biochem Biophys.* 2002; 408:131–136. [PubMed: 12485611]
- Zoncu R, Bar-Peled L, Efeyan A, Wang S, Sancak Y, Sabatini DM. mTORC1 senses lysosomal amino acids through an inside-out mechanism that requires the vacuolar H(+)-ATPase. *Science.* 2011; 334:678–683. [PubMed: 22053050]

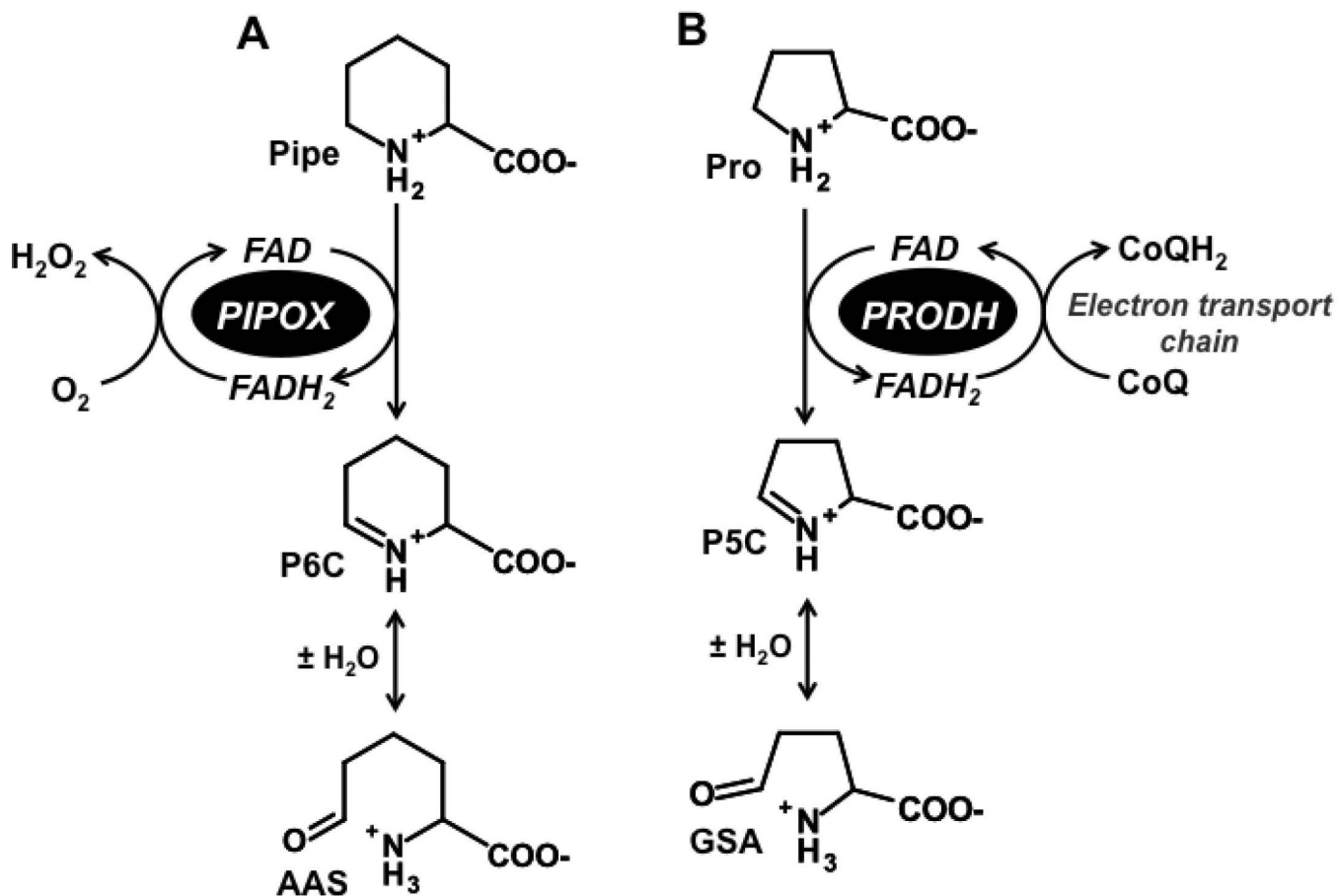


**Figure 1. Reactions catalyzed by pipecolate oxidase and proline dehydrogenase**  
 (A) Pipecolate oxidase (PIPOX) catalyzes the oxidation of L-pipecolate (Pipe) to <sup>1</sup>-piperidine-6-carboxylate (P6C). P6C spontaneously hydrolyzes to form  $\alpha$ -aminoadipic semialdehyde (AAS). (B) In an analogous reaction, proline dehydrogenase (PRODH) catalyzes the oxidation of L-proline (Pro) to <sup>1</sup>-pyrroline-5-carboxylate (P5C), which spontaneously hydrolyzes to glutamate  $\gamma$ -semialdehyde (GSA).



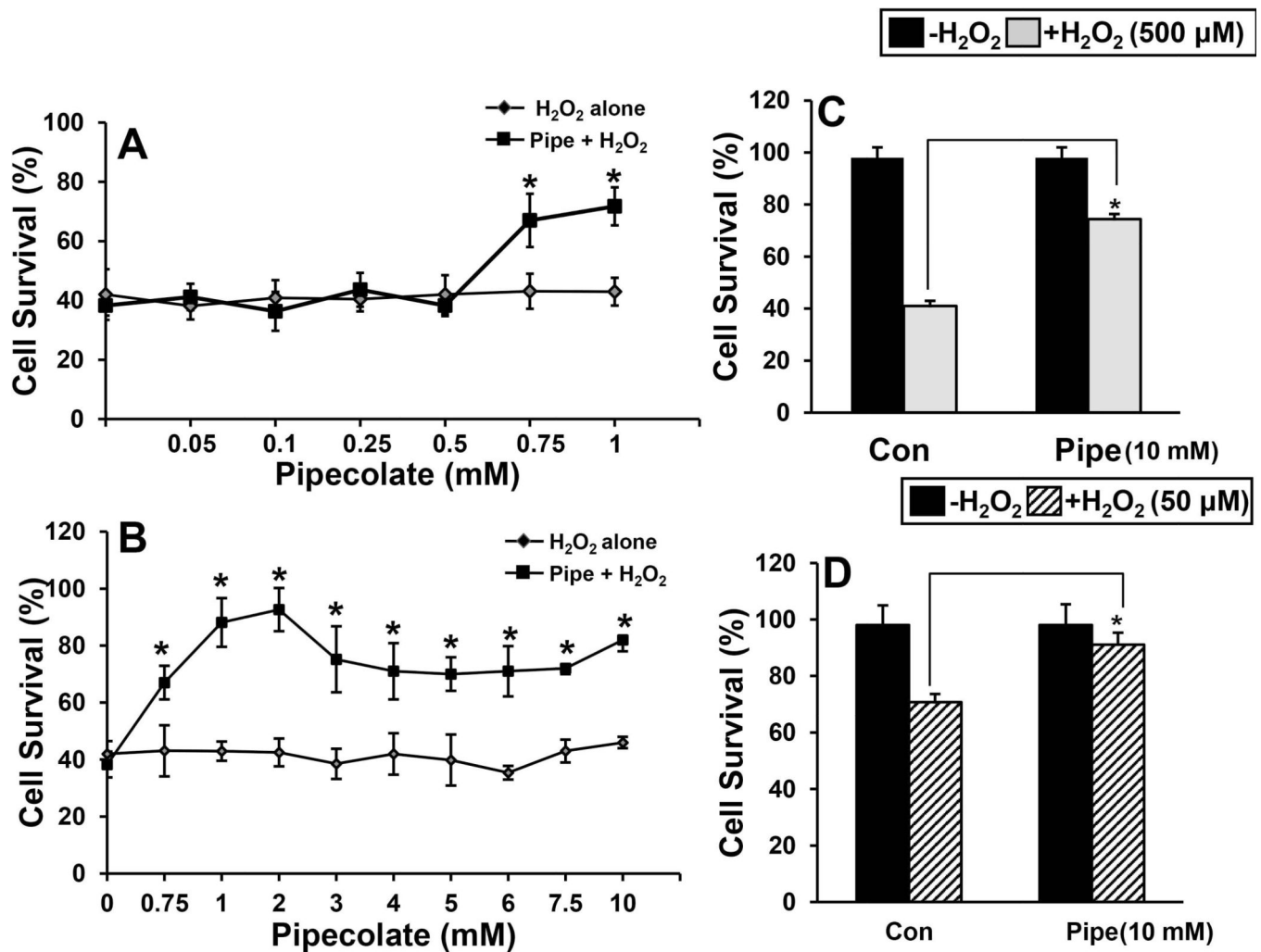


**Figure 2. Oxidative stress protection of HEK293 cells by pipercolate**

(A) HEK293 cells were treated without pipercolate (Con) and with different concentrations of pipercolate (Pipe) for 12 h (0.05–1 mM). Control and pipercolate treated cells were then incubated in serum free medium with and without 0.5 mM H<sub>2</sub>O<sub>2</sub> for 3 h. Percent cell survival was estimated using the MTS cell viability assay. (B) HEK 293 cells were treated with or without pipercolate (0.75–10 mM) for 12 h. Control and pipercolate treated cells were then incubated in serum free medium with and without 500 μM H<sub>2</sub>O<sub>2</sub> for 3 h. Percent cell survival was estimated using the MTS cell viability assay. (C) HEK293 cells treated with and without pipercolate (10 mM) for 12 h. Control and pipercolate treated cells were then incubated in serum free medium with and without 500 μM H<sub>2</sub>O<sub>2</sub> for 3 h. Percent cell survival was determined using the Cell Titer-Glo Luminescent assay. (D) HEK293 cells were treated as above. Control and pipercolate (10 mM) treated cells were then incubated in serum free medium with and without 50 μM H<sub>2</sub>O<sub>2</sub> for 3 h. Percent cell survival was determined using the Cell Titer-Glo Luminescent assay. Each value represents mean ± SD from five different experiments (n = 5) (\**P* < 0.05).

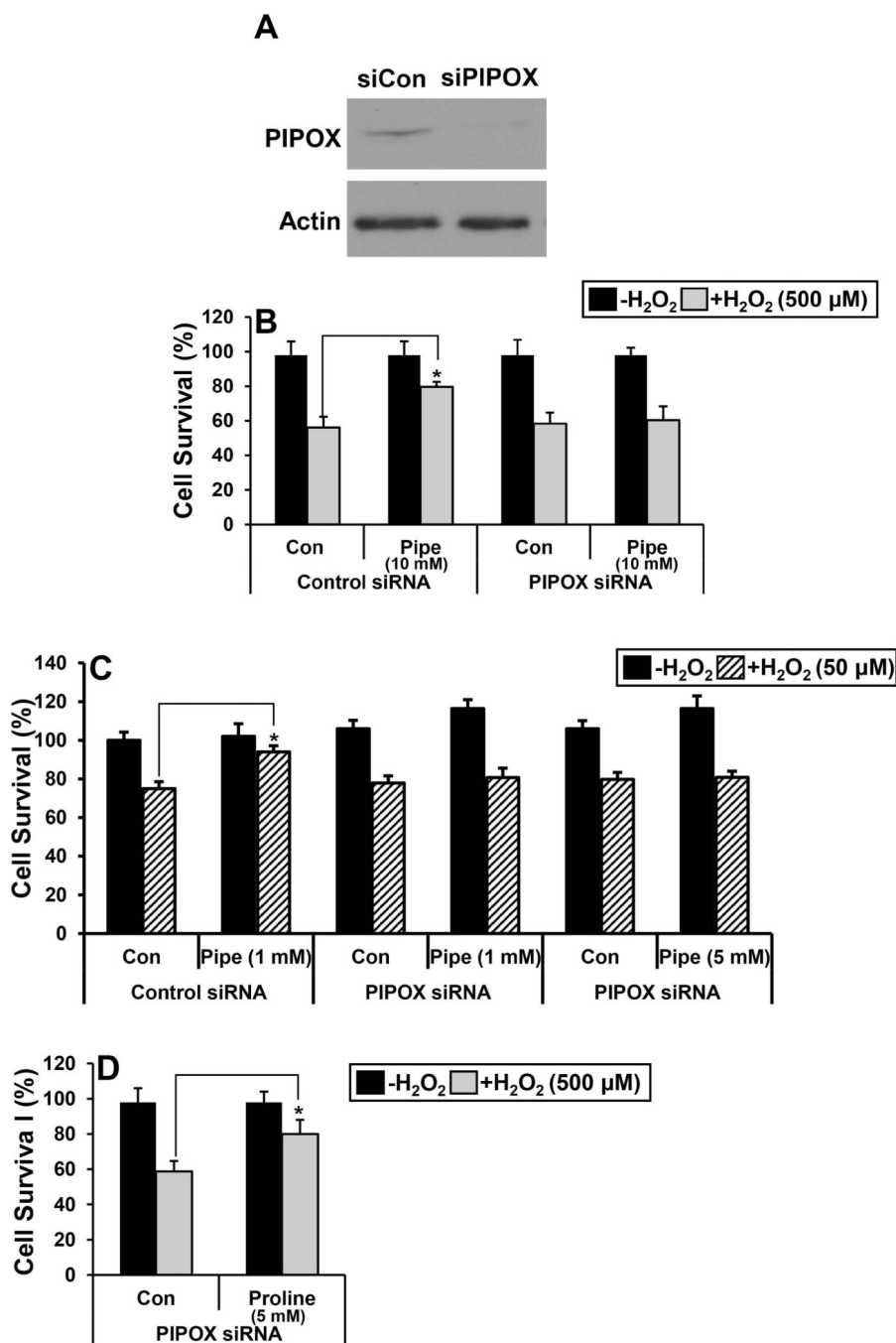


**Figure 3. Knockdown of PIPOX abolishes pipecolate protection**

(A) Western blot analysis of PIPOX in HEK293 cells transfected with control siRNA (siCon, 100 nM) and PIPOX siRNA (siPIPOX, 100 nM) for 48 h. Actin was used as a control. (B) Percent cell survival of control siRNA (siCon) or PIPOX siRNA (siPIPOX) treated HEK293 cells with and without 0.5 mM H<sub>2</sub>O<sub>2</sub> (3 h) in the absence (Con) and presence of 10 mM pipecolate (Pipe). (C) Percent cell survival of control siRNA or PIPOX siRNA treated HEK293 cells with and without 50 μM H<sub>2</sub>O<sub>2</sub> (3 h) in the absence (Con) and presence of 1 mM or 5 mM pipecolate (Pipe). (D) Percent cell survival of control siRNA (siCon) or PIPOX

siRNA (siPIPOX) treated HEK293 cells with and without 500  $\mu\text{M}$   $\text{H}_2\text{O}_2$  (3 h) in the absence (Con) and presence of 5 mM proline. Percent cell survival in all experiments was estimated using the MTS cell viability assay. Each value represents mean  $\pm$  SD of separate experiments (n = 5) (\* $P$  < 0.05).

Author Manuscript

Author Manuscript

Author Manuscript

Author Manuscript

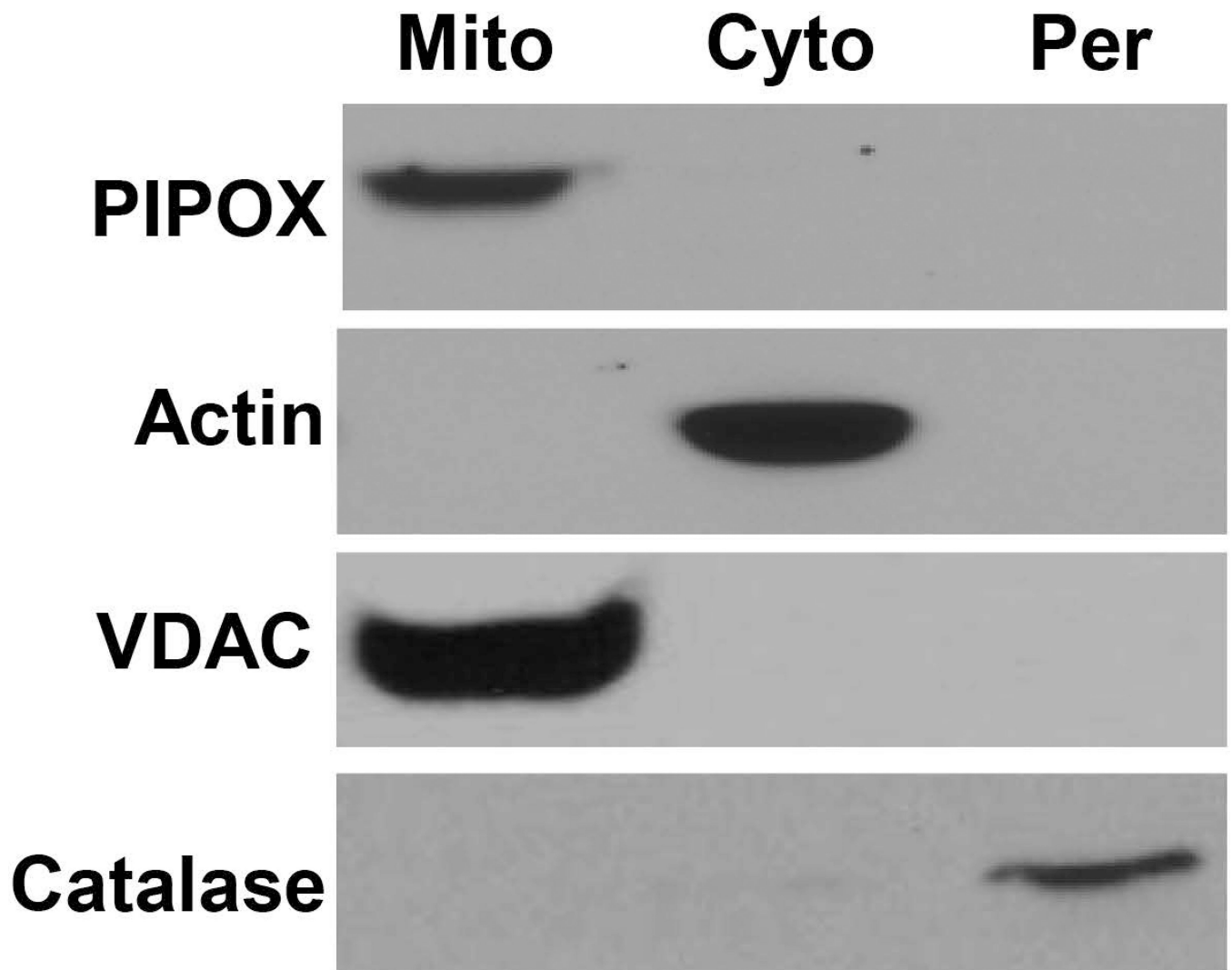


**Figure 4. Subcellular localization of PIPOX**

Immunoblot analysis of PIPOX in mitochondria, peroxisomes, and cytosolic fractions isolated from HEK293 cells. Actin, VDAC and catalase visualized with respective antibodies were used as fraction-specific markers for cytosol (Cyto.), mitochondria (Mito.) and peroxisomes (Per.), respectively.

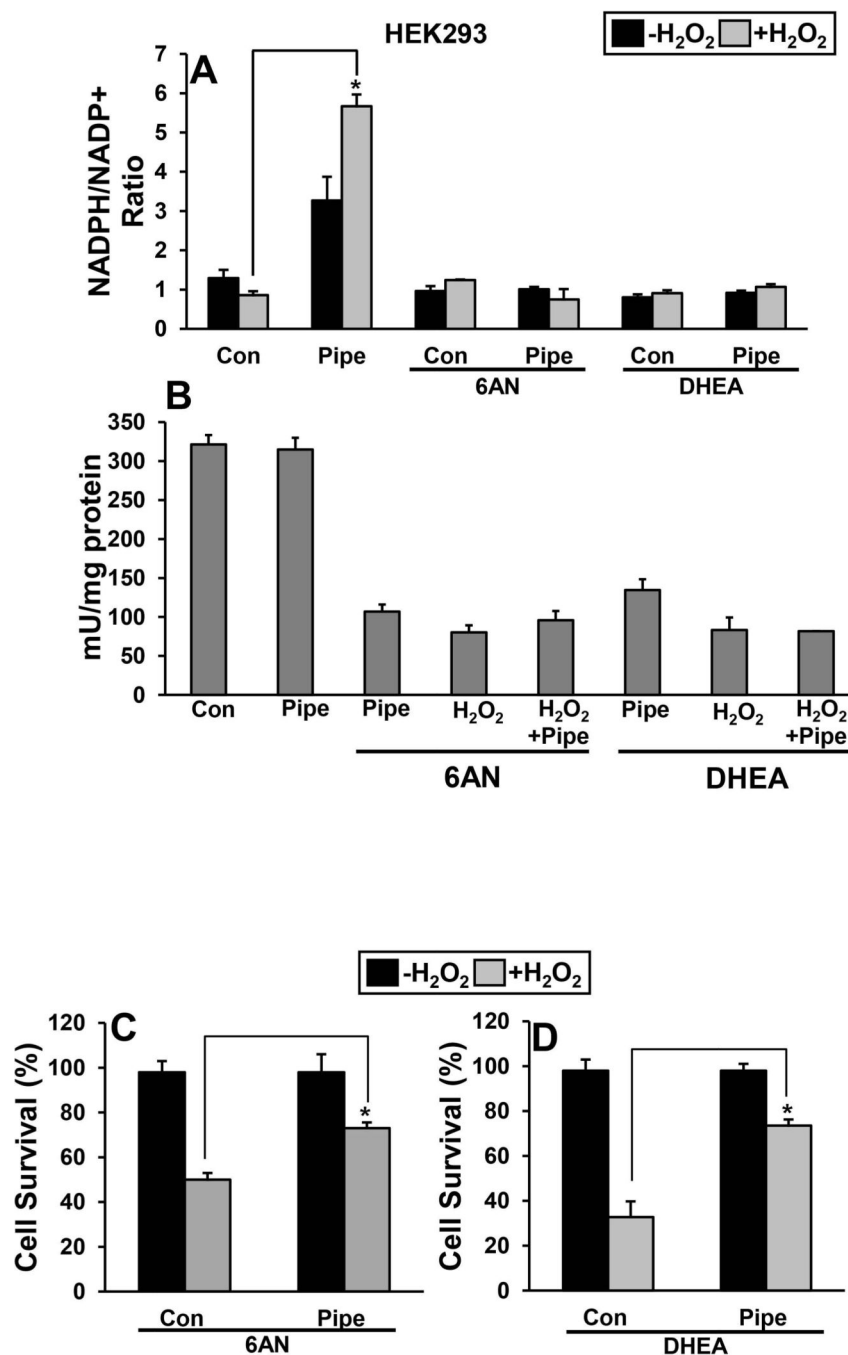


**Figure 5. Effect of piperolate on intracellular NADPH/NADP<sup>+</sup> ratio**

(A) The ratio of NADPH/NADP<sup>+</sup> was determined for control (Con) and piperolate-treated (Pipe, 10 mM) HEK293 cells with and without 500  $\mu$ M H<sub>2</sub>O<sub>2</sub> (3 h). The NADPH/NADP<sup>+</sup> ratio was also estimated in cells incubated in the presence of 6AN or DHEA. Each value represents mean  $\pm$  SD of separate experiments (n = 5) (\**P* < 0.05). (B) Glucose 6-phosphate dehydrogenase activity in HEK293 cells under different treatments. Percent survival of HEK 293 cells first treated with 6-amino nicotinamide (6-AN) (C) and dehydroepiandrosterone

(DHEA) (D). Percent cell survival was estimated using the MTS cell viability assay. Each value represents mean  $\pm$  SD of separate experiments (n = 5) (\*  $P < 0.05$ ).

Author Manuscript

Author Manuscript

Author Manuscript

Author Manuscript



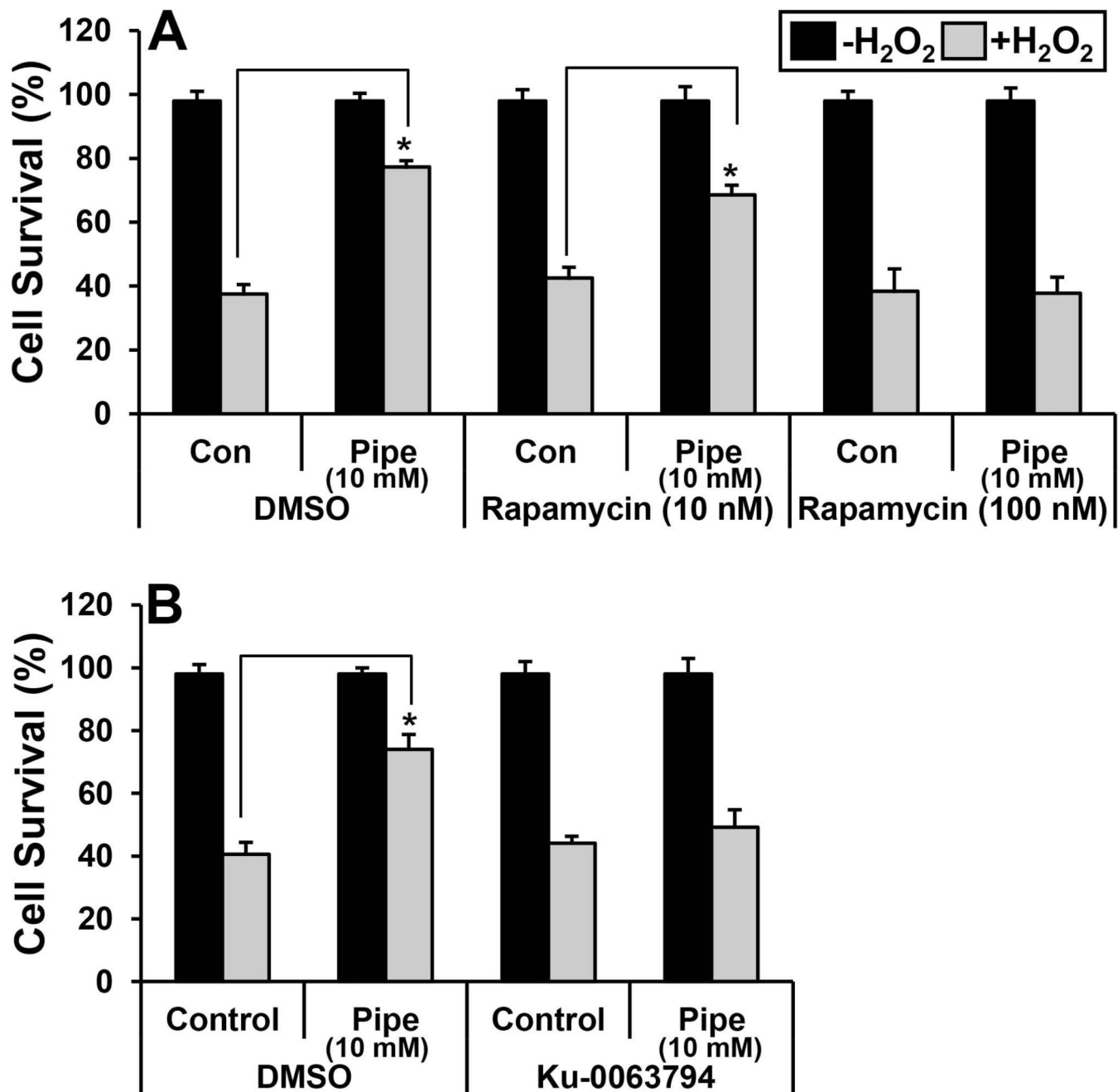


**Figure 6. Inhibition of mTORC2 blocks pipecolate protection**

(A) Percent cell survival of HEK293 cells incubated with rapamycin (10 nM and 100 nM) and treated with and without 0.5 mM H<sub>2</sub>O<sub>2</sub> (3 h) in the absence (Con) and presence of 10 mM pipecolate (Pipe). (B) Percent cell survival of HEK293 cells incubated with Ku-0063794 (10 nM) and treated with and without 0.5 mM H<sub>2</sub>O<sub>2</sub> (3 h) in the absence (Con) and presence of 10 mM pipecolate (Pipe). Cells treated with DMSO were used as controls. Percent cell survival was estimated using the MTS cell viability assay. Each value represents mean  $\pm$  SD of separate experiments (n = 5) (\*  $P < 0.05$ ).

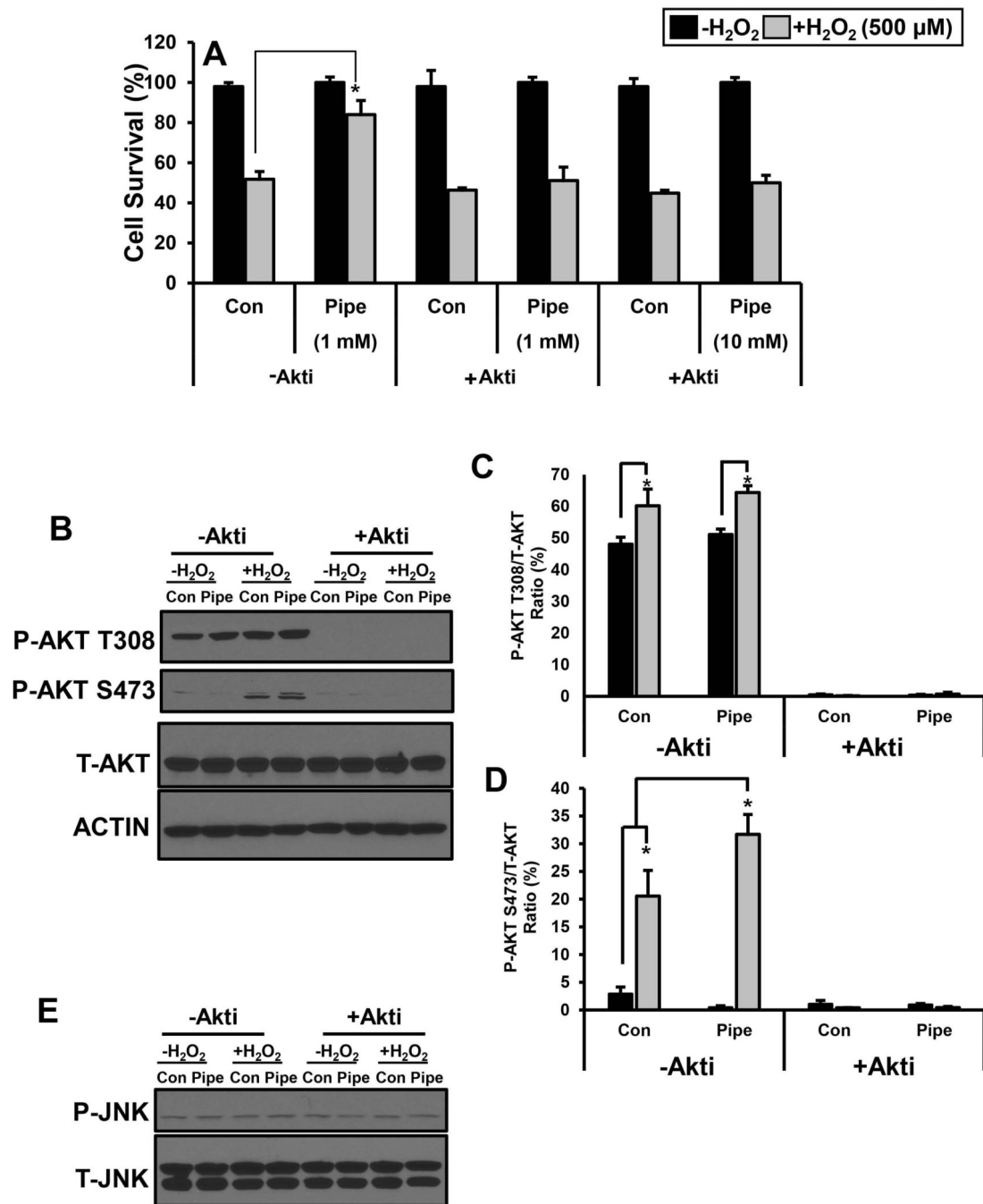


**Figure 7. Role of Akt in pipecolate protection**

(A) Percent cell survival of HEK293 cells incubated without Akti (–Akti) or with 10 μM Akti (+ Akti) and treated with and without 500 μM H<sub>2</sub>O<sub>2</sub> stress (3 h) in the absence (Con) and presence of 1 mM or 10 mM pipecolate (Pipe). Cells treated with DMSO were used as controls. Percent cell survival was estimated using the MTS cell viability assay. Each value represents mean ± SD of separate experiments (n = 5) (\* *P* < 0.05). (B) Western analysis of P-Akt (T308 and S473), T-Akt and Actin in HEK293 cells treated with and without pipecolate (1 mM) for 12 h and then incubated with and without 0.5 mM H<sub>2</sub>O<sub>2</sub> for 0.5 h in

serum free medium. Western analysis of P-Akt and T-Akt were also determined in cells with similar treatment conditions but in the presence of 10  $\mu$ M Akt inhibitor (+ Akti). Quantified levels of (C) P-Akt (T308) and (D) P-Akt (S473) relative to total Akt (P-Akt/Akt). (E) Western analysis of P-JNK, and T-JNK in HEK293 cells treated with and without pipercolate (1 mM) for 12 h and then incubated with and without 0.5 mM H<sub>2</sub>O<sub>2</sub> for 0.5 h in serum free medium. Western analysis of P-JNK and T-JNK were also determined with similar treatment conditions but in the presence of 10  $\mu$ M Akt inhibitor (+ Akti). Blots shown are representative results from three independent experiments. Each value represents the mean  $\pm$  SD of separate experiments (n = 3) (\*  $P < 0.05$ ).

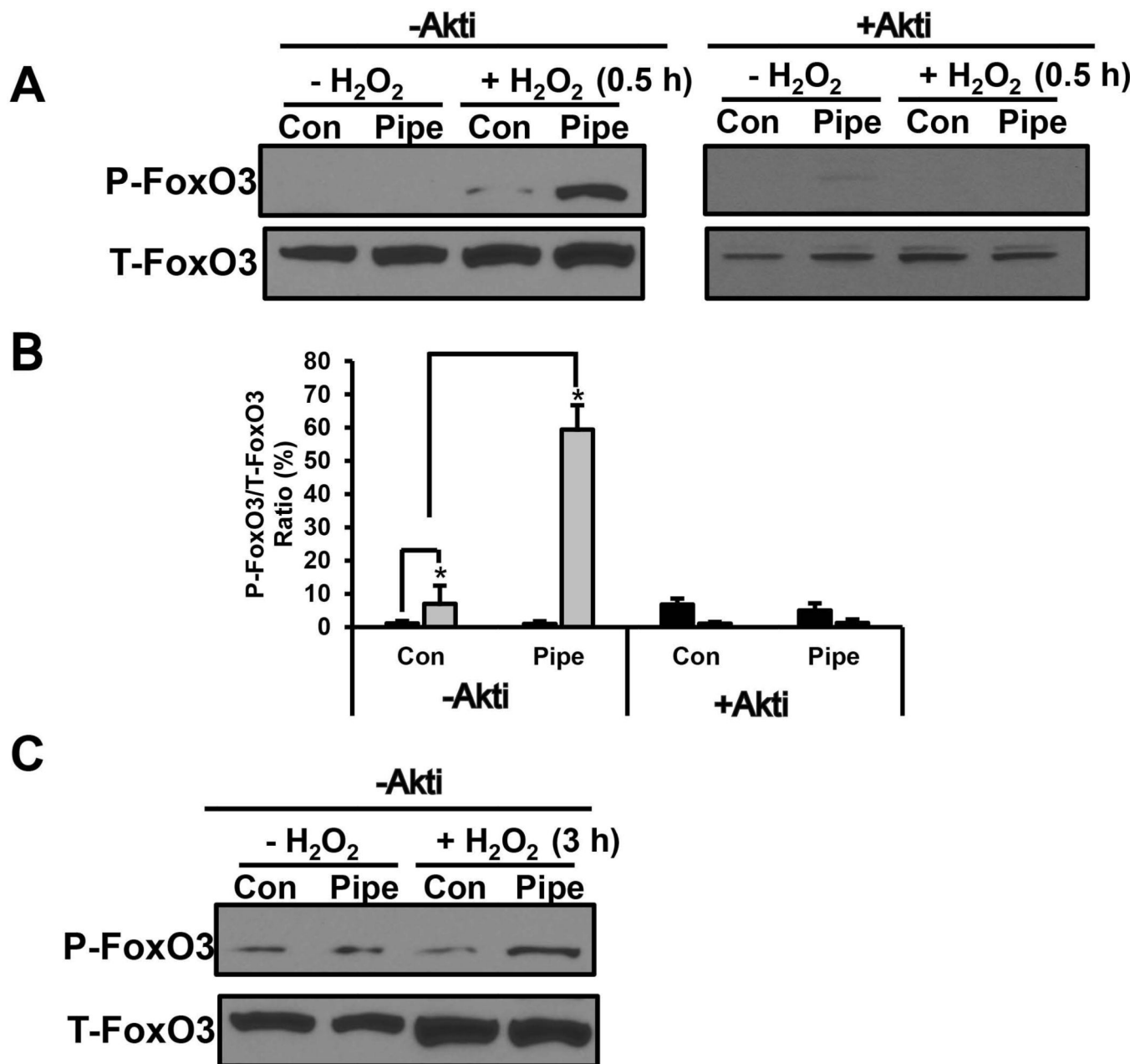


**Figure 8. Involvement of FoxO3 in pipecolate protection**

(A) Western analysis of P-FoxO3 (P-Thr32) and T-FoxO3 (total FoxO3) in HEK293 cells treated with and without pipecolate (1 mM) for 12 h and then incubated with and without 0.5 mM H<sub>2</sub>O<sub>2</sub> for 0.5 h in serum free medium. Blots are shown for experiments performed in the absence (– Akti) and presence (+Akti) of 10 μM Akt inhibitor (B) Quantified levels of P-FoxO3 (T32) relative to T-FoxO3 from Western blots as described in panel A in the absence (– Akti) and presence (+ Akti) of Akt inhibitor. (C) Same as in panel A but incubated with and without 0.5 mM H<sub>2</sub>O<sub>2</sub> for 3 h in serum-free medium. Blots shown are representative

results from three independent experiments. Each value represents the mean  $\pm$  SD of separate experiments (n = 3) (\*  $P < 0.05$ ).

Author Manuscript

Author Manuscript

Author Manuscript

Author Manuscript